

Unsupervised detection of semantic correlations in big data

Santiago Acevedo,^{1,*} Alex Rodriguez,^{2,3,†} and Alessandro Laio^{1,3,‡}

¹*International School for Advanced Studies (SISSA),*

Via Bonomea 265, 34136 Trieste, Italy

²*Dipartimento di Matematica e Geoscienze, Università degli Studi di Trieste,*

via Alfonso Valerio 12/1, 34127 Trieste, Italy

³*The Abdus Salam International Centre for Theoretical Physics (ICTP),*

Strada Costiera 11, 34014 Trieste, Italy

Abstract

In real-world data, information is stored in extremely large feature vectors. These variables are typically correlated due to complex interactions involving many features simultaneously. Such correlations qualitatively correspond to semantic roles and are naturally recognized by both the human brain and artificial neural networks. This recognition enables, for instance, the prediction of missing parts of an image or text based on their context. We present a method to detect these correlations in high-dimensional data represented as binary numbers. We estimate the *binary intrinsic dimension* of a dataset, which quantifies the minimum number of independent coordinates needed to describe the data, and is therefore a proxy of semantic complexity. The proposed algorithm is largely insensitive to the so-called curse of dimensionality, and can therefore be used in big data analysis. We test this approach identifying phase transitions in model magnetic systems and we then apply it to the detection of semantic correlations of images and text inside deep neural networks.

*Electronic address: sacevedo@sissa.it

†Electronic address: alejandro.rodriuezgarcia@units.it

‡Electronic address: laio@sissa.it

Correlations among the features defining a data point force a data set to live in a manifold \mathcal{M} whose geometry encodes the correlation structure of data. The most fundamental property of \mathcal{M} is its *intrinsic dimension*[1] which is qualitatively defined by the number of independent variables needed to parameterize it without significant information loss. If one was able to estimate the intrinsic dimension in a generic big data scenario, one would be able to quantify the strength of correlations in real-world datasets, like a corpus of sentences or a large set of measurements from a camera. However, real-world data are represented in feature spaces that are outrageously large, and most of the available methods meet serious problems if the intrinsic dimension of the manifold is of the order of hundreds or more[2]. We developed an intrinsic dimension estimator that generalizes the concept of the intrinsic dimension to the case of binary variables. We show that this allows circumventing the curse of dimensionality, and estimating reliably the intrinsic dimension even when it is of order 100,000. This result paves the way to a plethora of applications, allowing to address questions which have thus far been, to the best of our knowledge, intractable. For example, we can measure the range of semantic correlations in a corpus of sentences with hundreds of words, and we demonstrate that these correlations are destroyed when shorter, unrelated sentences are joined together. We show that our approach is effective in a variety of other fields and topics, from the study of phase transitions and of frustration-induced disorder in statistical physics, to image classification.

Detecting and quantifying correlations in generic real-world data is a complex task since features live in high dimensional spaces and have interactions of arbitrary range and nature. For example, in an image, the meaning of a scene can emerge from the simultaneous presence of two objects that are physically far away. Moreover, semantic correlations are often associated with collective effects, such as the simultaneous presence of three or more specific objects. A prominent example where non-trivial correlations emerge is the feature space of deep neural networks. Those spaces typically lack a well-defined order, and neurons that are close in the architecture are not necessarily coding related information. This hinders the direct interpretability of those feature spaces, leading many scientists, even today, to consider neural networks as "black boxes".

The main idea of this work is to use the intrinsic dimension (ID) of a dataset to detect and quantify correlations. If, for example, in a long text correlations between the first and the

second part of the text vanish, the ID of the whole text should be approximately equal to the sum of the ID of the two parts. More precisely, in data points including features describing independent information, the ID should scale *linearly* with the number of features N , namely $ID = \gamma N$ for some positive constant γ . If one would be able to estimate the ID as a function of text length (or as a function of the patch dimension, in the case of images) one would be able to detect the *range* of the correlation. Moreover, the difference between the sum of the IDs of two representations and the ID of a dataset composed by the concatenation of these representations provides a quantitative measure of the *strength* of the correlations[3]: for perfectly correlated representations the ID of the concatenation will be equal to the ID of the single representations.

However, most of the available algorithms to perform ID estimation meet serious problems if the intrinsic dimension of the manifold is of the order of hundreds or more[2]. In particular, some of them fail to provide an estimate of the ID which scales linearly with the number of features even when those are generated independently. Indeed, methods relying on the statistics of local neighborhoods systematically underestimate the ID because the number of samples required to sample a dataset grows exponentially in the ID[4]. This problem is a manifestation of the so-called *curse of dimensionality*[5] and affects to different extent all the ID estimators we are aware of, even if recently some progress has been made[6].

In order to estimate the ID in very large feature spaces, we here renounce to develop a general-purpose ID estimator, and we focus on features that are binary or can be approximately considered as binary. Concretely, we developed an ID estimator for binary data, called BID (from Binary Intrinsic Dimension) which, as we show below, can cope numerically with extremely large dimensionalities. Binary variables are the basis of all digital computation but are also of fundamental importance in both theoretical and applied science. The so-called spin systems, in which a spin is a binary degree of freedom, provide standard models to understand phases of matter, such as spin glasses[7], and spin liquids[8], and the corresponding phase transitions, like spontaneous ordering[9]. Binary variables are also used to describe biological neurons[10, 11] or social dynamics[12]. In artificial neural networks, the activations are typically real numbers, but many efforts focus on finding more efficient representations: the so-called quantization methods[13, 14] aim to represent activations or weights using small integer numbers or binary variables, in order to drastically save memory, energy, and computing time, while preserving performance. Activations and

weights can be transformed in binary variables by the sign function[15, 16]. Binarization has been shown to preserve the scalar product between the activations and weights[17]. In Supp. Inf. we show that binarization also approximately preserves the local neighbourhoods computed using the full-precision activations inside a Large Language Model (LLM). This suggests that binarizing in high dimensions is an operation that retains relevant information about the data[18].

In the following, we introduce an algorithm that can be used to estimate the binary intrinsic dimension (BID) of very large datasets of binary variables. We first show that it provides estimates that scale approximately linearly with system size when the system can be split into subsystems that are statistically independent, and reliably estimates the intrinsic dimension for bit streams of length up to $L \sim O(10^6)$, even using only $O(1000)$ samples. We benchmark the algorithm on model systems in which the binary variables interact with an explicit energy function, which allows modulating their correlations. We show that the dependence of the BID on system size allows for characterizing the nature of correlations between the variables and spotting the transitions between ordered and disordered phases. We finally apply this approach to the study of the internal representations of images and text in large neural networks.

Our algorithm is based on a generalization of exact results for distance distributions between statistically independent binary variables. Let $\sigma \in \mathcal{C} = \{0, 1\}^N$ be a string of N independent bits, and let each bit be uniformly distributed in $\{0, 1\}$. Then, the probability of observing a Hamming distance r between two configurations σ and σ' is

$$P_0(r) = \frac{1}{2^N} \binom{N}{r}. \quad (1)$$

Geometrically, the coordinates of uncorrelated random bits are points uniformly distributed in the N -dimensional configuration space \mathcal{C} , and the intrinsic dimension d coincides with the number of variables, N . If one would measure the empirical distribution of the hamming distance, by following a procedure akin to the one used in ref.[19], one could infer the value of N by the shape of such a distribution. However, such a procedure would fail if the bits are correlated since the empirical distribution would not match the theoretical distribution in eq. 1 for any value of N . In the case of correlated spins, we assume that the dimension

is a smooth function of the distance r , and therefore make the following ansatz:

$$P(r) = C \frac{1}{2^{d(r)}} \binom{d(r)}{r}, \quad (2)$$

where C is the normalization constant. Eq. (2) reduces to (1) for $d(r) = N$ and $C = 1$. We empirically found that model (2) fits accurately the observed distributions, at least locally, if one retains the first two terms of the Taylor expansion:

$$d(r) = d_0 + d_1 r \quad (3)$$

where d_0 and d_1 are variational parameters. In Supp. Inf. we show a Maximum Likelihood Estimation approach to infer a scale-dependent BID that supports our assumption of linear dependence (3).

In order to infer d_0 and d_1 we minimize the Kullbac-Leibler divergence between the empirical probability of Hamming distances $P_{emp}(r)$ and the model $P(r)$ given by Eqs. (2) and (3),

$$D_{KL}(P_{emp}||P) = \sum_{r \leq r^*} P_{emp}(r) \log \frac{P_{emp}(r)}{P(r)}, \quad (4)$$

where r^* is a meta-parameter that allows constraining the fit to small distances (see Supp. Inf.). As a representative measure of the BID of a system, we consider the limit for small distances of $d(r)$, which qualitatively corresponds to the local number of degrees of freedom. According to Eq. (3), we simply have $BID \equiv d_0$.

To benchmark our approach we use spin systems from statistical physics (summarized in Fig. 1). In those systems, the variables are spins which can take two values (up or down) and which, therefore, are binary variables. By choosing an interaction law between the spins, one can generate sets of binary variables correlated in highly non-trivial manners. The spins (or bits) are generated by sampling through standard Monte Carlo techniques[20] the Boltzmann distribution $P(\boldsymbol{\sigma}) \propto \exp(-\beta E(\boldsymbol{\sigma}))$, being E the energy function encoding the interactions between spins and $\beta = 1/T$ the inverse temperature.

We first show that our algorithm is able to compute intrinsic dimensions that scale linearly with size when the input data consists of statistically independent subsystems. We generated 2500 bit streams by concatenating B blocks of $N = 10^4$ bits, where each block is generated by independently harvesting spins from a Boltzmann distribution at $T = 2$, with an energy

function $E(\boldsymbol{\sigma}) = \sum_{i=1}^{N=1} \sigma_i \sigma_{i+1}$ with periodic boundary conditions ($\sigma_{N+1} \equiv \sigma_1$). Table I shows that the BID per bit is approximately constant from 10^4 bits to 10^6 bits, consistent with the system being constructed by concatenating independent blocks. Remarkably, the approach allows estimating intrinsic dimensions of order 10^5 using only 2500 data points. This is empirical evidence that the estimator proposed in this work is not affected by the curse of dimensionality, and can be used in extremely high dimensional spaces.

Number of blocks (B)	1	10	100
Number of bits (L)	10^4	10^5	10^6
BID	8047	80497	804624
BID per bit	0.8047	0.8050	0.8046
log(KL divergence)	-9.2	-8.2	-7.1

TABLE I: **BID linear scaling with system size for i.i.d concatenated blocks of bits.**

Next, we show that the BID is capable of capturing correlations between bits even when those span very large distances. We consider spins harvested from the Boltzmann distribution of the two-dimensional ferromagnetic Ising model on the square lattice (see Supp. Inf. for details). At high temperatures, spin-spin correlations are short-range, namely, they decay exponentially fast with the lattice distance. The characteristic scale of these correlations, the correlation length $\xi(T)$, is much smaller than the system size $L = \sqrt{N}$, implying that the BID must be asymptotically proportional to the number of bits. This is observed in the curve corresponding to $T = 4.0$ in Fig. 1A. The value of the BID per bit is close to 1, reflecting the presence of small correlations. The same behavior is observed at $T = 3$, with a relative BID that is smaller, consistently with the fact that correlations become more important. At low temperatures, the system is globally ordered (namely the majority of bits are either 0 or 1) but the fluctuations are also short-range correlated[21]. Thus the BID is again proportional to the number of bits, but its value is much lower, reflecting the presence of a dominant strong correlation between the variables "forcing" most of the bits to align. Near the critical temperature ($T = 2.3$) the relative BID does not reach a plateau, indicating that the correlation length is comparable with the size of the system. This is a well-known phenomenon observed in spin systems at criticality[21], which is captured by the BID through the sub-linear scaling with the number of bits. Fig. 1D shows the BID

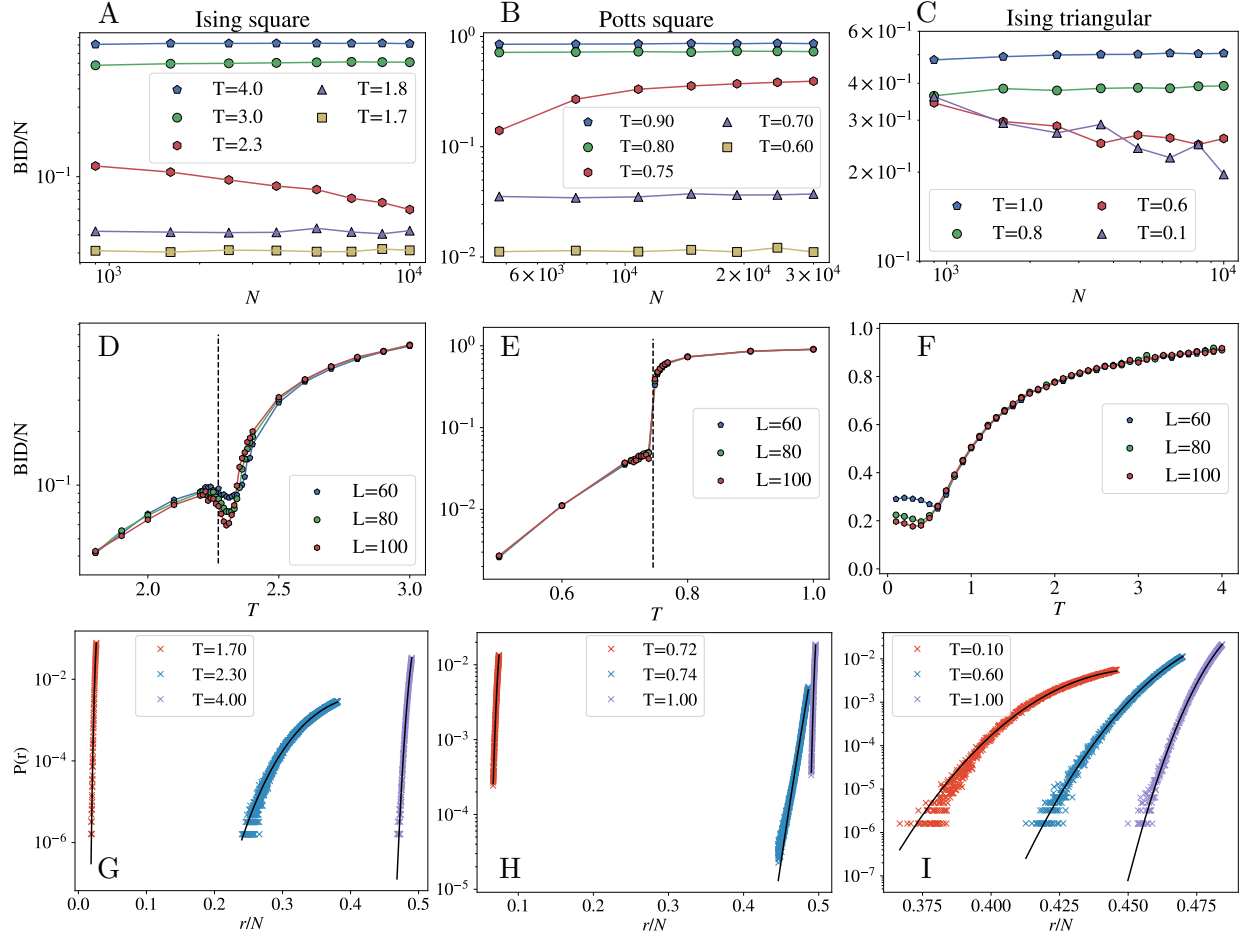


FIG. 1: **The BID of spin systems as models of interacting bit arrays.** Upper row: BID per spin as a function of the total number of spins N , for several temperatures T . Central row: Thermal dependence of the BID normalized per spin. L stands for the lattice width (or height). Bottom row: Model validation at $L = 100$ and different temperatures. (A,D,G): ferromagnetic Ising model on the square lattice, (B,E,H): the Potts model on the square lattice with $q = 8$ states, (C,F,I): the antiferromagnetic Ising model on the triangular lattice. On vertical dashed lines the exact results in the thermodynamic limit for (D) the critical temperature, $T_c = 2/\log(1 + \sqrt{2})$ and (E) the transition temperature $T^* = 1/\ln(1 + \sqrt{q}) \approx 0.745$.

as a function of temperature for the 2D ferromagnetic Ising model. Away from criticality, the BID per spin tends smoothly to zero or one as the temperature goes to zero or infinity, respectively. The critical temperature is easily recognized in the graph since, consistently with ref. [22], we observe a local minimum of the BID at that temperature.

The second system we studied is a q -state Potts model, with $q = 8$ (see Supp. Inf. for

details). In order to calculate its BID we construct a binary system by writing the state (or color) index q in a binary representation. The correlation length in this model has a maximum at the transition temperature but remains finite even in the thermodynamic limit[23]. This behavior is correctly captured by the BID scaling being asymptotically linear for every temperature (Fig. 1B), even close to the transition temperature T^* . The BID shows an abrupt change around T^* , consistent with the underlying first-order thermal phase transition.

Finally, we considered the Ising model on the triangular lattice with antiferromagnetic first-neighbor interactions. Due to geometrical frustration, this model does not have a thermal phase transition but presents a smooth crossover towards a ground state that has an entropy proportional to the number of spins in the system[24] and moreover presents a power-law decay of correlations[25]. Fig. 1C captures the long-range correlations of the ground-state through the sublinear scaling of the BID per bit, only present at small temperatures. Decreasing the temperature, the BID per spin tends smoothly to a non-zero value for all system sizes studied (Fig. 1F). The bottom panels in Fig. 1 illustrate the viability of the model defined in eq. Eqs 2 and 3 to describe the observed histograms of the distances between bit streams in all the conditions considered in the tests: the black lines, corresponding to the model of Eq. 2, fit pretty accurately the observations in all the conditions, even if at different temperatures the observations are concentrated at very different distances.

These benchmark examples show that BID is able to characterize the collective behavior of a large number of bits. Analogously, in computer vision, the collective behavior of a large number of pixels gives rise to patterns, which encode the meaning of an image. We computed the BID of internal representations of a convolutional image classifier, constructing binary data representations simply using the sign of the real-valued activations (see Supp. Inf. for details). The BID behaves as a proxy of semantic content, as we show through the following size-scaling experiment. The first row of Fig. 2 shows an example of different crops for one element of ImageNet, where each crop is resized to the fixed full-image resolution. Fig. 2 shows how the BID of the representations inside Resnet18 depends on the initial crop size, for different layers. For small crop sizes the BID increases monotonically, since on average the semantic content related to the classification task is being added. For large enough crop sizes, the BID saturates, indicating that all the relevant content of the image was

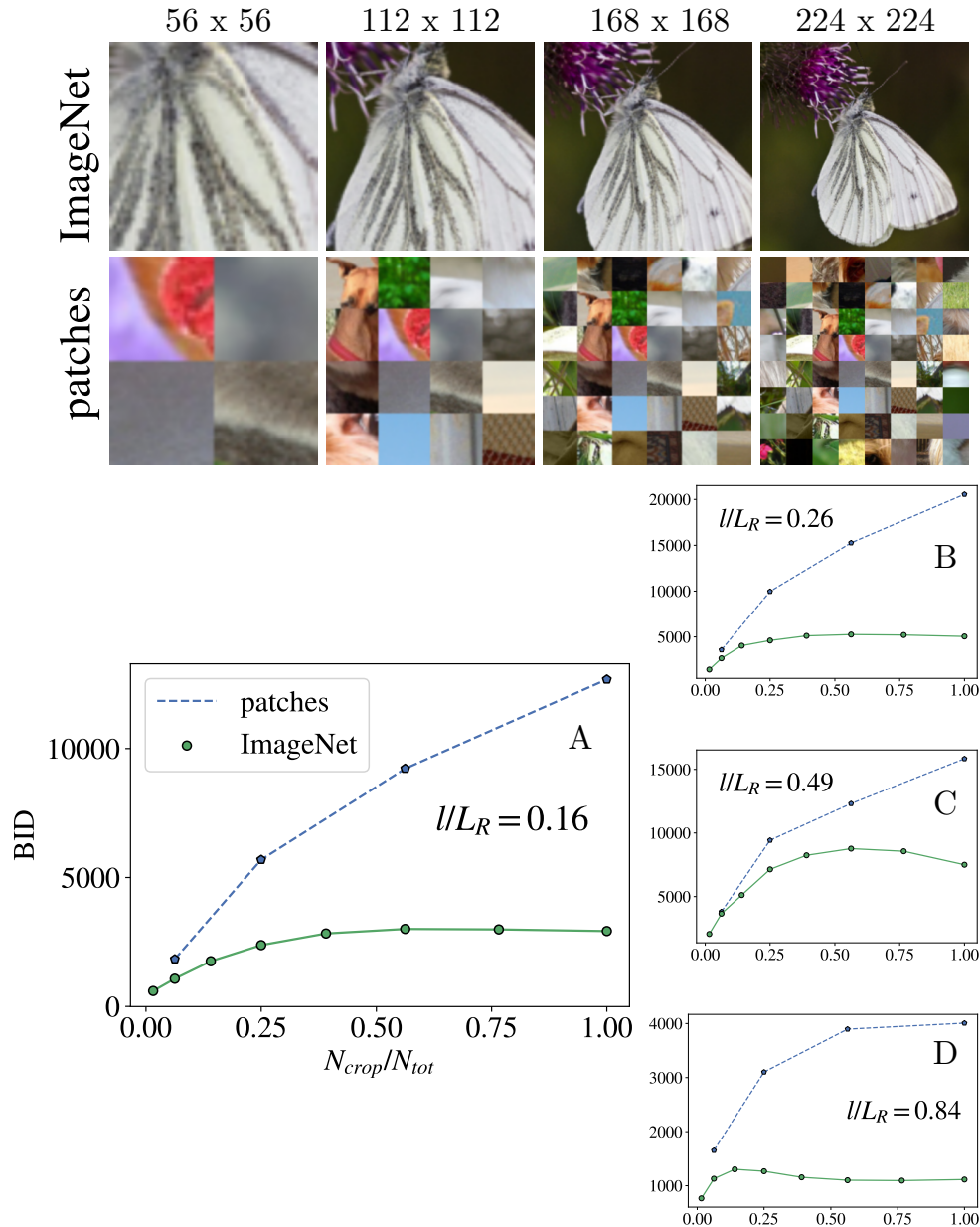


FIG. 2: **The BID of image-crop representations in Resnet18.** Upper row of images: example of crops for a sample of ImageNet. On top of each image, we report the size of the crop. All images are resized to 224×224 resolution after cropping, thus the rightmost image is the full image. Lower row of images: a set of images constructed from random patches of size 28×28 from ImageNet samples. A, B, C, D panels: BID of image representations as a function of the number of pixels in the cropped image, N_{crop} , where we normalized the latter by dividing by the total number of pixels in the full image, $N_{tot} = 224^2$. For each panel, l is the layer index and L_R is the total number of layers. For further details see Supp. Inf.

already present in previous sizes. Later layers saturate earlier since they carry information that is only relevant for the classification task and on average adding more context does not make significant changes. Indeed, if we consider a sufficiently small crop of a generic image, it is not possible to assign a label to it, since it does not carry enough information to make a discrimination. Instead, semantic information emerges for big enough crop sizes but saturates when the crop is so large that the extra pixels do not bring new information. In Fig. 2 we also show the same analysis performed on images constructed by an ensemble of random patches of the same data set. In this case, the semantic content is lost, even if the local structure in the images is preserved. Consequently, the BID does not plateau, since large images correspond to a collection of independent crops, each bringing the addition of independent information.

As a last example, we show that the BID can be used to detect correlations in the feature maps learned by large transformer-based architectures trained on a natural language processing (NLP) task. The ID has been used to analyze the properties of deep autoregressive transformers for protein sequence analysis and image analysis[26] and more recently for language [27, 28]. However, to make the ID estimation possible in Ref. [26] the representations were averaged in the sequence dimension, mixing information associated with the different tokens. In Refs. [27, 28], the analyses are performed only on the representation of the last token. We here use our approach to estimate the binary intrinsic dimension of the representation of whole sentences, probing in this manner the collective properties of all the neurons of a layer. We consider paragraphs from Wikitext consisting of more than 300 tokens, and we study how the BID scales with text length, binarizing activations through the application of the sign function. The initial representation (layer 0, Fig. 3, left panel) has short-range correlations, signaled by the BID per bit slowly drifting up as a function of the number of tokens (Fig. 3). Token embeddings are correlated because they must be compliant with the grammar structure of natural language, in which words are often used in groups. For long sentences, the BID scales approximately linearly with the sentence length: grammar-related correlations become less relevant in parts of a sentence separated by hundreds of words. Instead, the BID per bit of the last-layer representation learned by the model displays a clear power-law decay as a function of the number of tokens, similar to the one observed in scale-free critical spin systems (see Fig. 1A). Since the semantic content in text is a collective property of the whole sentence, the network to capture this property develops a long-range

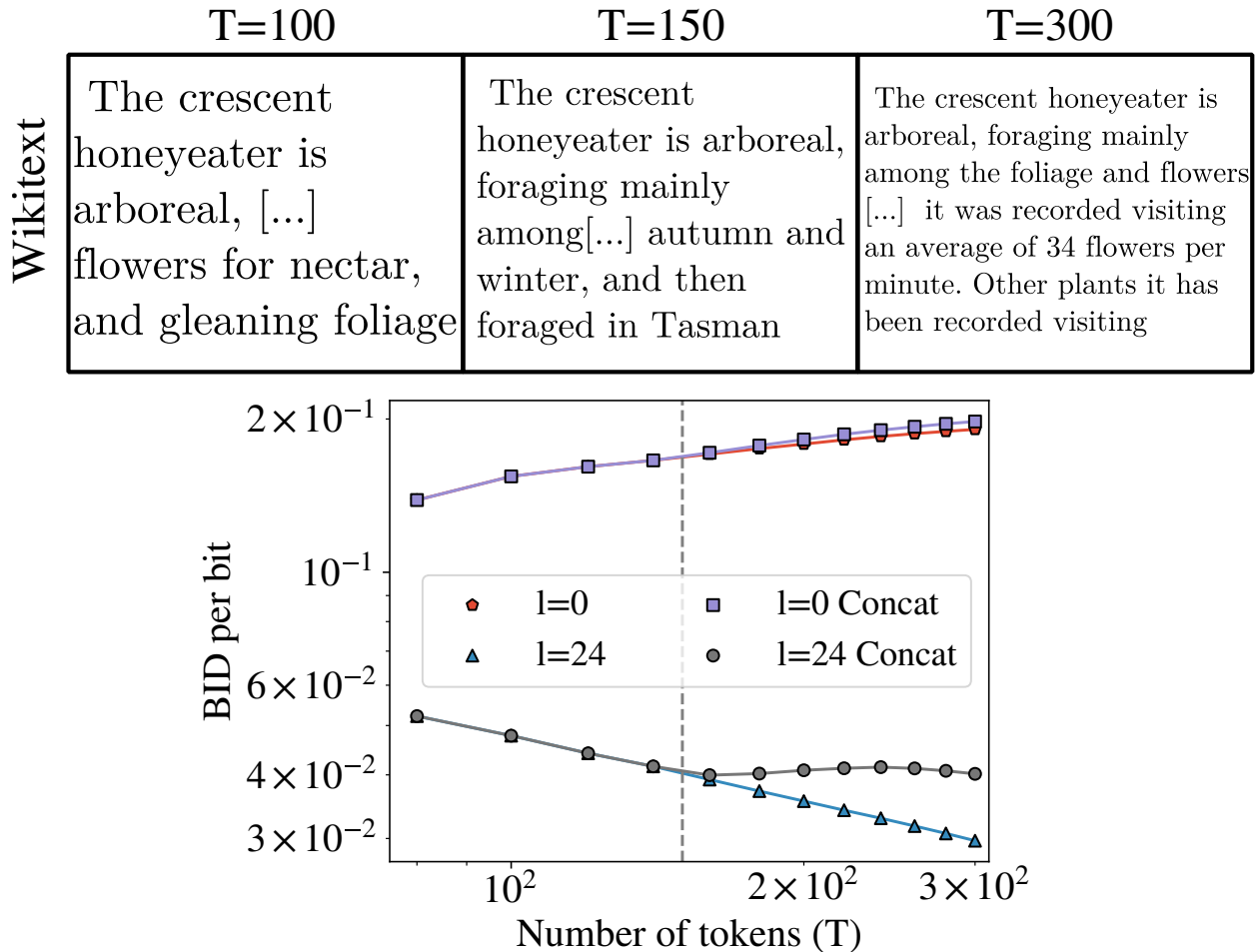


FIG. 3: **The BID of text representations in large language models.** Upper boxes: an example of a Wikitext sentence truncated at different token lengths, T . Central panel: BID per bit calculated using all token representations in the sequence as a function of the number of tokens, for Pythia410m (see Supp. Inf. for details). $l = 0$ stands for the embedding layer, $l = 24$ corresponds to the last transformer layer before the head. "Concat" stands for phrases constructed concatenating 150 tokens from two randomly selected data samples. The dashed line corresponds to the semantic boundary between the two phrases.

correlated representation: qualitatively the process of understanding the meaning of a long sentence can be described as the process of finding meaningful correlations in the sequence of tokens. To validate that we are indeed capturing the semantic correlations in text through the BID scaling we repeat the experiment by concatenating 150 tokens from two randomly

chosen sentences from the same corpus. We observe that the power law decrease stops precisely at the boundary between phrases, and it is followed by an approximate plateau, consistent with the two halves of the paragraph containing independent information. In the last part of the plot, the BID per bit starts decreasing again, as a result of the semantic correlations of the second half of the sentence. In Supp. Inf. we show that these results hold also for changing both corpus and network.

These findings are aligned with pioneering studies that have suggested power-law correlations between characters in human text but were numerically limited due to the difficulty of computing mutual information in high dimensions[29, 30]. Moreover, the critical behavior of activations complies with the more recent observation of neural scaling laws[31] where the loss function of autoregressive transformers decreases as a power-law of the number of parameters. Also consistent with our results, a recent work observed a critical phase transition in GPT-2, with the temperature parameter appears in the autoregressive sampling[32]. To make computations feasible, the authors restricted the representation space to that of Part-Of-Speech (POS) tags only.

In conclusion, we introduced an intrinsic dimension estimator specifically designed for binary data. To the best of our knowledge, the only other estimator for such variables was recently introduced in the context of formal concept analysis [33]. However, it has only been benchmarked on simple binary data tables, whereas our approach is tailored for large bit streams. We tested examples with up to 10^6 bits without observing systematic errors in the scaling of the estimation with system size.

The spin system benchmarks demonstrate that our estimator can characterize the global correlation structure of different phases of matter and identify the corresponding phase transitions. When applied to data representations from deep neural networks, the scaling of BID allows us to infer correlations for both image recognition and language modeling tasks. In the case of image classification, the BID behaves as a proxy of semantic content, since it initially increases with image-crop size after which it plateaus, indicating no additional information is gained from extra pixels. Instead, for images constructed out of independent random patches this plateau does not take place. For sentences, the correlations extend throughout the text and the BID of the last transformer layer follows a power law when computed using representations from a real corpus. In contrast, in an artificial corpus generated by concatenating real sentences, these correlations break, showing that the power

law is inherent to the data and not an artifact of our estimator.

It is noteworthy that the last two datasets consist of real-valued features, while the BID estimator is designed for binary data. Each feature was converted into a binary variable by taking its sign. In Supp. Inf. we show that the trends observed in Fig. 3 hold when using two bits per feature instead of one. Specifically, the relative BID estimated for this higher-precision representation scales with the same power law. This suggests that when the intrinsic dimension becomes extremely large (around 1000 or more), its trends are insensitive to the precision used to represent individual features, and binning retains the essential information of the representation, as suggested in Refs. [13, 15].

The BID of data representations is clearly not restricted to either images or text, which are taken here as use cases where semantic correlations are easily interpretable. We expect our algorithm to be useful in the analysis of generic high dimensional spaces where global correlations are unknown, for example data coming from stock markets or brain activity. In perspective it would be interesting to explore its relationship with the Shannon entropy estimated by compression algorithms[34].

Acknowledgements

The authors acknowledge Marco Baroni, Antonello Scardicchio and Marcello Dalmonte for useful discussions.

Code and data availability

The code used to obtain the results of this work can be found in <https://github.com/acevedo-s/BID>. Routines to compute the BID are implemented in the open-source package DADApY[35].

-
- [1] R. Bennett. The intrinsic dimensionality of signal collections. *IEEE Transactions on Information Theory*, 15(5):517–525, 1969. doi: 10.1109/TIT.1969.1054365.
 - [2] Francesco Camastra and Antonino Staiano. Intrinsic dimension estimation: Advances and open problems. *Information Sciences*, 328:26–41, 2016.

- [3] Lorenzo Basile, Santiago Acevedo, Luca Bortolussi, Fabio Anselmi, and Alex Rodriguez. Intrinsic dimension correlation: uncovering nonlinear connections in multimodal representations, 2024.
- [4] J.-P. Eckmann and D. Ruelle. Fundamental limitations for estimating dimensions and lyapunov exponents in dynamical systems. *Physica D: Nonlinear Phenomena*, 56(2):185–187, 1992. ISSN 0167-2789. doi: [https://doi.org/10.1016/0167-2789\(92\)90023-G](https://doi.org/10.1016/0167-2789(92)90023-G). URL <https://www.sciencedirect.com/science/article/pii/016727899290023G>.
- [5] C.M. Bishop. *Pattern Recognition and Machine Learning*. Information Science and Statistics. Springer New York, 2016. ISBN 9781493938438. URL <https://books.google.it/books?id=kOXDtAEACAAJ>.
- [6] Vittorio Erba, Marco Gherardi, and Pietro Rotondo. Intrinsic dimension estimation for locally undersampled data. *Scientific reports*, 9(1):17133, 2019.
- [7] K. Binder and A. P. Young. Spin glasses: Experimental facts, theoretical concepts, and open questions. *Rev. Mod. Phys.*, 58:801–976, Oct 1986. doi: 10.1103/RevModPhys.58.801. URL <https://link.aps.org/doi/10.1103/RevModPhys.58.801>.
- [8] Lucile Savary and Leon Balents. Quantum spin liquids: a review. *Reports on Progress in Physics*, 80(1):016502, nov 2016. doi: 10.1088/0034-4885/80/1/016502. URL <https://dx.doi.org/10.1088/0034-4885/80/1/016502>.
- [9] M. Kardar. *Statistical Physics of Fields*. Cambridge University Press, 2007. ISBN 9780521873413. URL <https://books.google.it/books?id=nTxBhGX01P4C>.
- [10] John J Hopfield. Neural networks and physical systems with emergent collective computational abilities. *Proceedings of the national academy of sciences*, 79(8):2554–2558, 1982.
- [11] A. Engel and C. Broeck. *Statistical Mechanics of Learning*. Statistical Mechanics of Learning. Cambridge University Press, 2001. ISBN 9780521774796. URL <https://books.google.it/books?id=qVo4IT9ByfQC>.
- [12] Claudio Castellano, Santo Fortunato, and Vittorio Loreto. Statistical physics of social dynamics. *Rev. Mod. Phys.*, 81:591–646, May 2009. doi: 10.1103/RevModPhys.81.591. URL <https://link.aps.org/doi/10.1103/RevModPhys.81.591>.
- [13] Itay Hubara, Matthieu Courbariaux, Daniel Soudry, Ran El-Yaniv, and Yoshua Bengio. Quantized neural networks: Training neural networks with low precision weights and activations. *Journal of Machine Learning Research*, 18(187):1–30, 2018.

- [14] Yunhui Guo. A survey on methods and theories of quantized neural networks. *arXiv preprint arXiv:1808.04752*, 2018.
- [15] Matthieu Courbariaux, Itay Hubara, Daniel Soudry, Ran El-Yaniv, and Yoshua Bengio. Binarized neural networks: Training deep neural networks with weights and activations constrained to+ 1 or-1. *arXiv preprint arXiv:1602.02830*, 2016.
- [16] Hongyu Wang, Shuming Ma, Li Dong, Shaohan Huang, Huaijie Wang, Lingxiao Ma, Fan Yang, Ruiping Wang, Yi Wu, and Furu Wei. Bitnet: Scaling 1-bit transformers for large language models. *arXiv preprint arXiv:2310.11453*, 2023.
- [17] Alexander G Anderson and Cory P Berg. The high-dimensional geometry of binary neural networks. *arXiv preprint arXiv:1705.07199*, 2017.
- [18] Aldo Glielmo, Claudio Zeni, Bingqing Cheng, Gábor Csányi, and Alessandro Laio. Ranking the information content of distance measures. *PNAS Nexus*, 1(2):pgac039, 04 2022. ISSN 2752-6542. doi: 10.1093/pnasnexus/pgac039. URL <https://doi.org/10.1093/pnasnexus/pgac039>.
- [19] Iuri Macocco, Aldo Glielmo, Jacopo Grilli, and Alessandro Laio. Intrinsic dimension estimation for discrete metrics. *Phys. Rev. Lett.*, 130:067401, Feb 2023. doi: 10.1103/PhysRevLett.130.067401. URL <https://link.aps.org/doi/10.1103/PhysRevLett.130.067401>.
- [20] M.E.J. Newman and G.T. Barkema. *Monte Carlo Methods in Statistical Physics*. Clarendon Press, 1999. ISBN 9780198517962. URL <https://books.google.it/books?id=KKL2nQEACAAJ>.
- [21] J.J. Binney, N.J. Dowrick, A.J. Fisher, and M.E.J. Newman. *The Theory of Critical Phenomena: An Introduction to the Renormalization Group*. Clarendon Press, 1992. ISBN 9780191660566. URL <https://books.google.it/books?id=BCOQDwAAQBAJ>.
- [22] T. Mendes-Santos, X. Turkeshi, M. Dalmonte, and Alex Rodriguez. Unsupervised learning universal critical behavior via the intrinsic dimension. *Phys. Rev. X*, 11:011040, Feb 2021. doi: 10.1103/PhysRevX.11.011040. URL <https://link.aps.org/doi/10.1103/PhysRevX.11.011040>.
- [23] E Buddenoir and S Wallon. The correlation length of the potts model at the first-order transition point. *Journal of Physics A: Mathematical and General*, 26(13):3045, 1993.
- [24] G. H. Wannier. Antiferromagnetism. the triangular ising net. *Phys. Rev.*, 79:357–364, Jul 1950. doi: 10.1103/PhysRev.79.357. URL <https://link.aps.org/doi/10.1103/PhysRev.79.357>.

- [25] Henk WJ Blöte and M Peter Nightingale. Antiferromagnetic triangular ising model: Critical behavior of the ground state. *Physical Review B*, 47(22):15046, 1993.
- [26] Lucrezia Valeriani, Diego Doimo, Francesca Cuturello, Alessandro Laio, Alessio Ansuini, and Alberto Cazzaniga. The geometry of hidden representations of large transformer models. In A. Oh, T. Naumann, A. Globerson, K. Saenko, M. Hardt, and S. Levine, editors, *Advances in Neural Information Processing Systems*, volume 36, pages 51234–51252. Curran Associates, Inc., 2023. URL https://proceedings.neurips.cc/paper_files/paper/2023/file/a0e66093d7168b40246af1cddc025daa-Paper-Conference.pdf.
- [27] Emily Cheng, Corentin Kervadec, and Marco Baroni. Bridging information-theoretic and geometric compression in language models. *arXiv preprint arXiv:2310.13620*, 2023.
- [28] Emily Cheng, Diego Doimo, Corentin Kervadec, Iuri Macocco, Jade Yu, Alessandro Laio, and Marco Baroni. Emergence of a high-dimensional abstraction phase in language transformers. *arXiv preprint arXiv:2405.15471*, 2024.
- [29] Wentian Li. Mutual information functions of natural language texts. Citeseer, 1989.
- [30] Werner Ebeling and Thorsten Pöschel. Entropy and long-range correlations in literary english. *Europhysics Letters*, 26(4):241, 1994.
- [31] Jared Kaplan, Sam McCandlish, Tom Henighan, Tom B. Brown, Benjamin Chess, Rewon Child, Scott Gray, Alec Radford, Jeffrey Wu, and Dario Amodei. Scaling laws for neural language models, 2020. URL <https://arxiv.org/abs/2001.08361>.
- [32] Kai Nakaishi, Yoshihiko Nishikawa, and Koji Hukushima. Critical phase transition in a large language model. *arXiv preprint arXiv:2406.05335*, 2024.
- [33] Tom Hanika and Tobias Hille. What is the *intrinsic* dimension of your binary data? – and how to compute it quickly, 2024. URL <https://arxiv.org/abs/2404.06326>.
- [34] Ram Avinery, Micha Kornreich, and Roy Beck. Universal and accessible entropy estimation using a compression algorithm. *Physical review letters*, 123(17):178102, 2019.
- [35] Aldo Glielmo, Iuri Macocco, Diego Doimo, Matteo Carli, Claudio Zeni, Romina Wild, Maria d’Errico, Alex Rodriguez, and Alessandro Laio. Dadapy: Distance-based analysis of data-manifolds in python. *Patterns*, 3(10):100589, 2022. ISSN 2666-3899. doi: <https://doi.org/10.1016/j.patter.2022.100589>. URL <https://www.sciencedirect.com/science/article/pii/S2666389922002070>.
- [36] Alessio Ansuini, Alessandro Laio, Jakob H Macke, and Davide Zoccolan. Intrinsic dimension

- of data representations in deep neural networks. *Advances in Neural Information Processing Systems*, 32, 2019.
- [37] . https://pytorch.org/hub/pytorch_vision_resnet/.
- [38] . https://pytorch.org/vision/stable/generated/torchvision.models.feature_extraction.get_graph_node_names.html.
- [39] Thomas Wolf, Lysandre Debut, Victor Sanh, Julien Chaumond, Clement Delangue, Anthony Moi, Pierric Cistac, Tim Rault, Rémi Louf, Morgan Funtowicz, et al. Huggingface’s transformers: State-of-the-art natural language processing. *arXiv preprint arXiv:1910.03771*, 2019.
- [40] D. Moltchanov. Distance distributions in random networks. *Ad Hoc Networks*, 10(6):1146–1166, 2012. ISSN 1570-8705. doi: <https://doi.org/10.1016/j.adhoc.2012.02.005>. URL <https://www.sciencedirect.com/science/article/pii/S1570870512000224>.

Supplementary Information

Optimization

The meta-parameter r^* is computed as the quantile of order α^* of the empirical probability of distances $P_{emp}(r)$, i.e., $\alpha^* = \sum_{r=0}^{r^*} P_{emp}(r)$, and we typically select the value of α^* that gives the lowest KL divergence (4). The minimization of (4) is performed stochastically, meaning we propose small random moves from (d_0, d_1) to $(d_0 + \delta_0, d_1 + \delta_1)$ for suitable δ_0 and δ_1 and we take them if they decrease the loss function, or reject them otherwise. When comparing BID's of a system computed with different model parameters (e.g., temperature, or size) we always do it at a shared value of α^* . Occasionally the smallest sampled distances are noisy and poorly sampled, which may induce overflow in the numerical minimization of (4), especially for very large bit streams. In this cases we introduce a regularizer r_{min} defined as the quantile of order α_{min} of P_{emp} to remove distances with $r < r_{min}$. Table II summarizes the values of these meta-parameters used in this work.

As an example we show additional optimization results for the 2D Ising model on the square lattice (Fig 1A,D,G from main text). Fig. 4 shows the thermal dependence of d_1 , $\log(KL)$ and r^* for different system sizes L . Notably d_1 has a maximum around T_c . Even if the error is maximum at T_c , the maximum of $\log(KL)$ is close to 10^{-7} , implying that the model fits accurately the data, as shown in Fig. 1G. r^* instead develops an inflexion point around T_c .

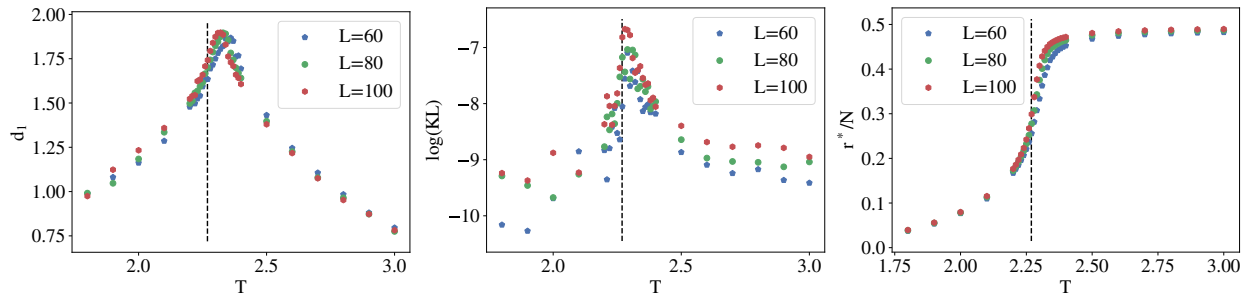


FIG. 4: Thermal dependence of d_1 , $\log(KL)$ and r^* for the 2D Ising model on the square lattice, $N = L^2$ stands for the total number of spins. The dashed line corresponds to the exact critical temperature in the thermodynamic limit.

Figure / Table	α_{min}	α_{max}
Table 1	0	1
Fig. 1A,D,G,B,E,H	0	.1
Fig. 1C,F,I	0	.05
Fig. 2	10^{-2}	0.5
Fig. 3,6,5	10^{-5}	.7

TABLE II: Meta-parameters used for figures and tables.

Spin systems

For every two dimensional spin model we sampled 5000 samples at each temperature with singly spin flip dynamics. We simulated each of the 5000 Markov chains independently in a different core with a different seed, so they are by construction independent from each other. For Ising models the algorithm used is Metropolis-Hastings, whereas for the Potts model we used the Heatbath algorithm[20]. For Table I we used 2500 samples.

Ising models

For all the Ising models simulated in this work, the energy of a given configuration of N spins $\boldsymbol{\sigma} = (\sigma_1, \dots, \sigma_N) \in \{-1, 1\}^N$ is

$$E(\boldsymbol{\sigma}) = -J \sum_{\langle i,j \rangle} \sigma_i \sigma_j, \quad (5)$$

with periodic boundary conditions, where $\langle i, j \rangle$ stands for first-neighbor interactions between spins i and j in the corresponding lattice. J Is the coupling constant between spins, fixed to +1 in the ferromagnetic models and -1 in the antiferromagnetic case.

Potts model

The energy of a given configuration $\boldsymbol{\sigma} = (\sigma_1, \dots, \sigma_N) \in \{0, 1, \dots, q-1\}^N$ is

$$E(\boldsymbol{\sigma}) = - \sum_{\langle i,j \rangle} \delta_{\sigma_i, \sigma_j}, \quad (6)$$

with periodic boundary conditions, where $q \in \mathbb{N}$ and δ stands for Kronecker delta. For $q > 4$ the system presents a first order phase transition. Since in this model all colors are equivalent, to improve the statistics we made a symmetry transformation making all simulations converge to the 0-ground state.

The BID of image representations

We followed the experimental setup of [36] by computing separately the BID of Resnet18 representations from 8 highly populated classes of ImageNet ('vizsla', 'koala', 'Shih-Tzu', 'Rhodesian_ridgeback', 'English_setter', 'cabbage_butterfly', 'Yorkshire_terrier'), where for each class we have roughly 1300 images. We measure the BID after each Resnet block, i.e., after each skip connection. Resnets have ReLU activation functions, so only two possible outputs of each unit are possible: zero or greater than zero. Taking the sign of such an output automatically constructs the binary system under the convention $sign(0) = 0$. The preprocessing of images was done following PyTorch official documentation[37]. The layer indexation was taken following the list of "graph_node_names", from the official PyTorch documentation[38].

The BID of text representations

Pretrained LLMs OPT350m and Pythia450m and associated tokenizers were downloaded from Huggingface[39], together with Wikitext and OpenWebtext corpora. Model architectures are available online. The activation function in the last fully connected layer of the transformer block in Pythia is GeLU, whereas in OPT the corresponding layer is linear (i.e., no activation function). Pythia450m has layer_norm before and after the self attention layer, whereas OPT350m has it between the attention block and the fully connected layers. Regardless of these details the binarization corresponds to take the sign of the activations (which in every layer have mean zero), and we see no qualitative difference when comparing results from Pythia on Wikitext to OPT on OpenWebtext (Fig. 5). Discarding sentences from Wikitext with less than 400 Tokens we kept around 7500 samples.

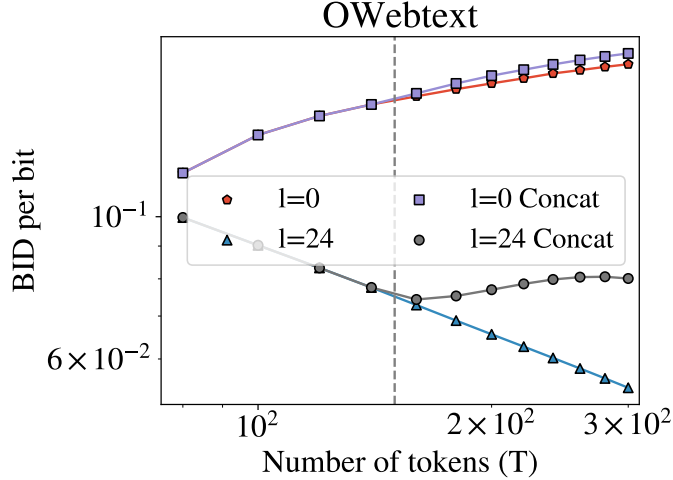


FIG. 5: BID per bit calculated using all token representations in the sequence as a function of the number of tokens, for OPT350m on OpenWebtext. $l = 0$ stands for the embedding layer, $l = 24$ corresponds to the last transformer layer before the head. "Concat" stands for phrases constructed concatenating 150 tokens from two randomly selected data samples. The dashed line corresponds to the semantic boundary between the two phrases.

To represent each activation of Pythia410m on Wikitext with 2 bits we proceed as follows. For each layer l we computed the mean μ^l , which is close to zero, and the standard deviation σ^l of the activations a_i^l , with $i = 1, \dots, N_a^l$ being N_a^l the number of activations in layer l . Then, we quantize the activations generating 2-bit variables σ_i^l by

$$\sigma_i^l = \begin{cases} 00 & \text{if } a_i^l < -\sigma^l \\ 01 & \text{if } -\sigma^l < a_i^l < 0 \\ 10 & \text{if } 0 < a_i^l < \sigma^l \\ 11 & \text{if } \sigma^l < a_i^l \end{cases} \quad (7)$$

Fig. 6 shows the comparison between sign binarization (Nbits=1) and the quantization (7) (Nbits=2).

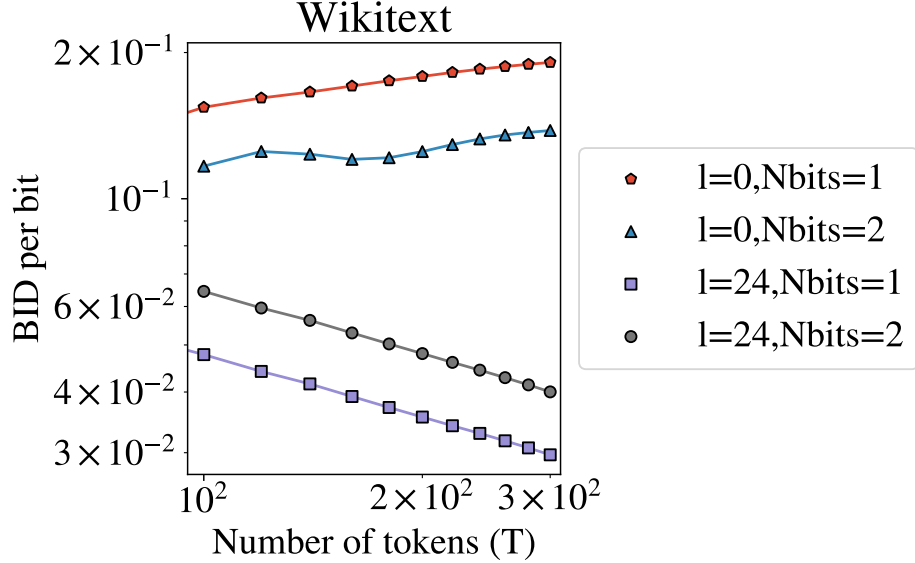


FIG. 6: Comparing BID size scalings using direct sign binarization (Nbits=1) or the binarization given by (7).

Maximum Likelihood Estimation of a scale-dependent BID

In this section we present a formal approach to define and estimate a scale-dependent BID, $d(r)$, that supports the ansatz (2) with the functional form (3). Following [19], we assume to have a Poisson process[40] in a generic domain in which we can define a set A and assign to it a volume, V_A . Assuming also to have a constant density of points ρ in A , the probability of observing n_A points falling inside A is

$$P(n_A, A) = \frac{(\rho V_A)^{n_A}}{n_A!} e^{-\rho V_A}, \quad (8)$$

such that $\langle n_A \rangle = \rho V_A$. We consider a data point $i \in A$, and another set B that contain A . Then, if the density is constant in set B ($\rho_A = \rho_B = \rho$) the conditional probability of having n_A points in A given that there are n_B points in B is

$$P(n_A|n_B) = \binom{n_B}{n_A} p^{n_A} (1-p)^{n_B-n_A}, \quad (9)$$

where $p \equiv V_A/V_B$. Note that this conditional probability does not depend on the density of points ρ . Then, the likelihood function is

$$\mathcal{L}(n_i|k_i, p_i) = \prod_{i=1}^{N_s} \text{Binomial}(n_i|k_i, p_i), \quad (10)$$

where N_s is the number of samples in the dataset. This equation is maximized to obtain the Maximum Likelihood Estimator \hat{d} . Doing this, in the limit of large number of samples, the equation that defines \hat{d} takes the form

$$\frac{V_A(\hat{d})}{V_B(\hat{d})} = \frac{\langle n_A \rangle}{\langle n_B \rangle}, \quad (11)$$

where $\langle n_A \rangle = \frac{1}{N_s} \sum_{i=1}^{N_s} n_A^i$, and the same for $\langle n_B \rangle$. To work specifically with Ising spin configurations $\boldsymbol{\sigma} \in \{-1, 1\}^N$ we depart from [19] using Hamming distances, which can be defined as

$$D_H(\boldsymbol{\sigma}, \boldsymbol{\sigma}') = \frac{N - \boldsymbol{\sigma} \cdot \boldsymbol{\sigma}'}{2} \quad (12)$$

The number of points at Hamming distance r from any Ising spin configuration in d dimensions is

$$V_H(r, d) = \sum_{r'=0}^r \binom{d}{r'} \quad (13)$$

where $r \in [0, d]$. At this point we have to choose specific sets A and B to estimate d . To favor the constant density ρ and constant dimension d on both sets, one can fix A to be the set of points at exactly distance r_A from the data point i , and B the set of points at distance r_A or $r_B = r_A + 1$. We denote this two sets as "thin shells". Given this choice, (11) has the close form solution

$$\frac{V_A}{V_B} = \frac{r_B}{d+1}, \quad (14)$$

for which the MLE for the ID is

$$\hat{d}(r_A) = \left((r_A + 1) \frac{\langle n_B \rangle}{\langle n_A \rangle} \right) - 1. \quad (15)$$

In order to interpret better the last equation, we observe that $\langle n_A \rangle \propto P(r = r_A)$, where $P(r)$ is the probability of observing hamming distance r between any two configurations in

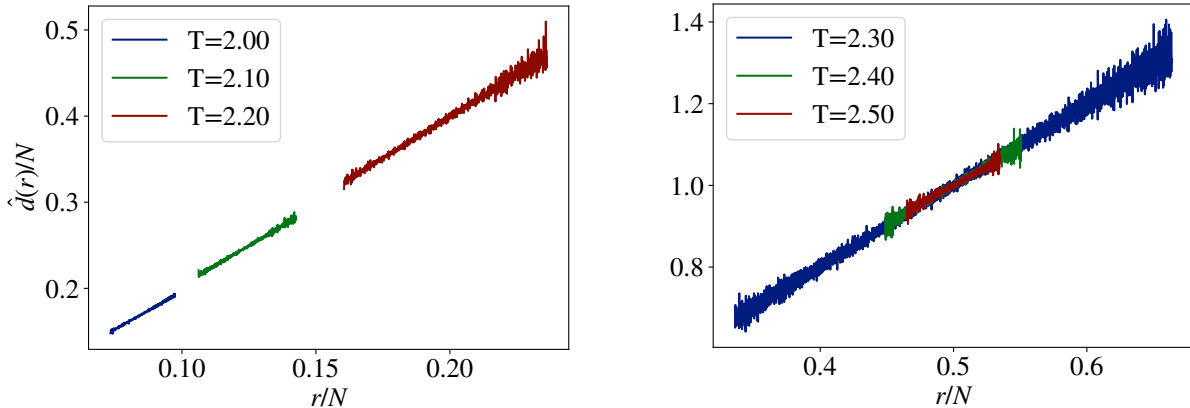


FIG. 7: Scale-dependent BID estimated by MLE (11) as a function of the observational scale r , on the two-dimensional ferromagnetic Ising model on the square lattice, for several temperatures T . Both axis are normalized by the total number of spins N in the system. The two panels are separated temperatures above (right) and below (left) the critical temperature of the system for visual clarity.

the dataset. Then,

$$\begin{aligned} \hat{d}(r_A) &\approx (r_A + 1) \frac{P(r = r_A) + P(r = r_A + 1)}{P(r = r_A)} - 1 = \\ &\approx (r_A + 1) \left(2 + \partial_r \log(P(r)) \Big|_{r=r_A} \right) - 1. \end{aligned} \quad (16)$$

where in the second step we did a first order Taylor expansion. Thus, given the empirical $P(r)$ this setup allows to estimate a scale-dependent intrinsic dimension from the slope of the log-probabilities at a given scale r_A .

Fig. 7 shows the scale dependence of the MLE (16) for the 2D Ising model where we observe a linear scale dependence in the whole range of probed scales, for every temperature. This linear dependence is consistent with the success of our ansatz (2) with a scale dependent $d(r)$ truncated to linear order (Eq. (3)). The scale-dependent BID (11) presents some drawbacks which are solved by the ansatz (2). First of all, there is no clear scale to select in either panel of Fig. 7, whereas by construction the coefficients of expansion (3) are scale independent. Furthermore, at high temperature (right panel of Fig. 7), for scales greater than $N/2$ the BID per bit becomes larger than 1, which is a paradox. We also observed this linear dependence of the BID as a function of the observational scale r studying ImageNet representations inside a Resnet. The results were noisy, since the MLE estimator uses the

slope of the empirical log probabilities at a given value of r . This led us to define our ansatz in the form of Eqs. (2) and (3) which is not noisy, since it fits the empirical histogram in a large range of scales.

Neighbourhoods are approximately preserved after binarizing high dimensional activations

In this section we study how the binarization of activations through the sign function affects the neighbourhood structures inside a LLM. To do this we start by considering the nearest neighbour of each data point in the full-precision space of activations generated by Pythia 410m on 6000 samples of Wikitext with 300 tokens each. For every such first neighbour we then compute its rank in the system of binarized activations. While in continuous space distances do not repeat and each rank is unique, for discrete systems this is no longer true and one has to choose a definition for the rank that takes this into account. In the following we consider that equidistant points share the rank.

Fig. 8 shows the distribution of ranks obtained after binarizing next-neighbour vectors of activations. For both initial (0) and last (24) layers the distributions are peaked at 1, meaning that the most probable rank after binarization is still 1 (i.e. first neighbours). Moreover, the expected rank after binarizing remains smaller than 10 in both cases, proving that ranks are approximately preserved after binarization. For the (unnormalized) initial layer we observed that subtracting the layer-mean was beneficial to concentrate the post-binarization rank distribution closer to 1.

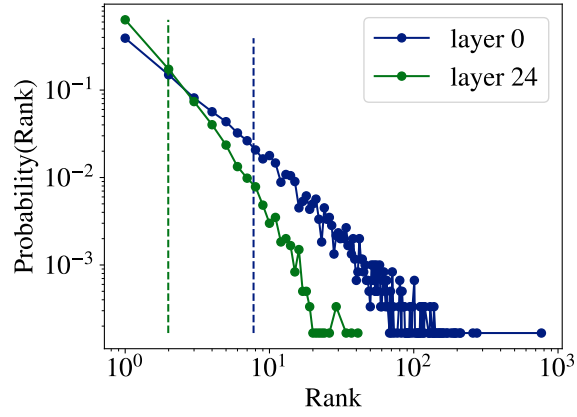


FIG. 8: Distribution of ranks obtained after binarizing the activations of a LLM, using points that were first neighbours in the full precision space. On vertical dashed lines the expected value of the distribution.